Vlasov simulation of electrostatic solitary structures in multi-component plasmas

Takayuki Umeda,[1] Maha Ashour-Abdalla,[2,3] Jolene S. Pickett,[4] and Melvyn L. Goldstein[5]

Received 20 September 2011; revised 9 February 2012; accepted 1 April 2012; published 16 May 2012.

[1] Electrostatic solitary structures have been observed in the Earth's magnetosheath by the Cluster spacecraft. Recent theoretical work has suggested that these solitary structures are modeled by electron acoustic solitary waves existing in a four-component plasma system consisting of core electrons, two counter-streaming electron beams, and one species of background ions. In this paper, the excitation of electron acoustic waves and the formation of solitary structures are studied by means of a one-dimensional electrostatic Vlasov simulation. The present result first shows that either electron acoustic solitary waves with negative potential or electron phase-space holes with positive potential are excited in four-component plasma systems. However, these electrostatic solitary structures have longer duration times and higher wave amplitudes than the solitary structures observed in the magnetosheath. The result indicates that a high-speed and small free energy source may be needed as a fifth component. An additional simulation of a five-component plasma consisting of a stable four-component plasma and a weak electron beam shows the generation of small and fast electron phase-space holes by the bump-on-tail instability. The physical properties of the small and fast electron phase-space holes are very similar to those obtained by the previous theoretical analysis. The amplitude and duration time of solitary structures in the simulation are also in agreement with the Cluster observation.

Citation: Umeda, T., M. Ashour-Abdalla, J. S. Pickett, and M. L. Goldstein (2012), Vlasov simulation of electrostatic solitary structures in multi-component plasmas, *J. Geophys. Res.*, *117*, A05223, doi:10.1029/2011JA017181.

1. Introduction

[2] The existence of Electrostatic Solitary Waves (ESWs) was first firmly established through observations made by the GEOTAIL spacecraft in the Earth's magnetotail [*Matsumoto et al.*, 1994]. These solitary waves have waveforms of bipolar electric field pulses longitudinal to the ambient magnetic field [*Kojima et al.*, 1997], which suggests that the solitary waves are electrostatic solitary structures. The electrostatic solitary structures are also observed in other regions of the Earth's magnetosphere: at the bow shock [*Bale et al.*, 1998], in the auroral region [*Mozer et al.*, 1997; *Ergun et al.*, 1998], in the polar cap boundary layer [*Franz et al.*, 1998], in the magnetotail magnetic reconnection region [*Cattell et al.*, 2005], at the magnetopause [*Cattell et al.*, 2002], and in the magnetosheath [*Pickett et al.*, 2003, 2005].

[3] There are two basic physical models proposed for the generation of electrostatic solitary structures. One of these interprets the solitary structures as electron phase-space holes and the other as electron acoustic solitary waves. Previous computer simulation studies demonstrated that electron phase-space holes are generated during the nonlinear evolution of weak-electron-beam (bump-on-tail) instabilities [*Omura et al.*, 1996; *Miyake et al.*, 1998; *Singh et al.*, 2000; *Umeda et al.*, 2002, 2004] and strong-electron-beam (two-stream) instabilities [*Goldman et al.*, 1999; *Miyake et al.*, 2000; *Oppenheim et al.*, 2001; *Umeda et al.*, 2006; *Umeda*, 2008a]. The electron phase-space holes correspond to positive potentials that trap electrons. They are modeled by using one-dimensional equilibrium solutions to the time-independent Vlasov-Poisson equations, [*Krasovsky et al.*, 1997, 2003; *Chen and Parks*, 2002; *Chen et al.*, 2004] which are called the Bernstein-Greene-Kruskal (BGK) equilibrium [*Bernstein et al.*, 1957].

[4] Recently, there has been an attempt to explain the electrostatic solitary structures as density structures (enhancements or decreases) which result from ion or electron acoustic instabilities [e.g., *Ghosh et al.*, 2008; *Lakhina et al.*, 2008, 2009, and references therein]. In the theoretical models of electron acoustic solitary waves, multicomponent plasma systems consisting of cold and hot electrons and one species of ions are assumed, and multifluid equations for each species are solved in a moving stationary frame. *Lakhina*

[1]Solar-Terrestrial Environment Laboratory, Nagoya University, Nagoya, Japan.
[2]Institute of Geophysical and Planetary Physics, University of California, Los Angeles, California, USA.
[3]Department of Physics and Astronomy, University of California, Los Angeles, California, USA.
[4]Department of Physics and Astronomy, University of Iowa, Iowa City, Iowa, USA.
[5]Laboratory for Geospace Science, NASA Goddard Space Flight Center, Greenbelt, Maryland, USA.

Corresponding author: T. Umeda, Solar-Terrestrial Environment Laboratory, Nagoya University, Nagoya, Aichi 464-8601, Japan. (umeda@stelab.nagoya-u.ac.jp)

0148-0227/12/2011JA017181

Table 1. Parameters for Different Simulation Runs

Run	ω_{pce}	V_{dce}	V_{tce}	ω_{ppe}	V_{dpe}	V_{tpe}	ω_{pae}	V_{dae}	V_{tae}	ω_{pi}	V_{di}	V_{ti}	ω_{pbe}	V_{dbe}	V_{tbe}
0	0.7484	0.0042	1.0	0.5023	1.3152	0.6685	0.4331	−1.3804	0.5435	0.0025	0.0	0.0344	–	–	–
1	0.7484	0.0042	1.0	0.5023	1.3152	0.4727	0.4331	−1.3804	0.3843	0.0025	0.0	0.0344	–	–	–
2	0.7484	0.0042	1.0	0.5023	1.3152	0.3342	0.4331	−1.3804	0.2717	0.0025	0.0	0.0344	–	–	–
3	0.7484	0.0042	1.0	0.5023	1.3152	0.6685	0.4331	−1.3804	0.5435	0.0025	0.0	0.0344	0.1	−2.2	0.1

et al. [2009] obtained solutions of positive solitary potentials by assuming four-component plasmas based on the Cluster observations in the magnetosheath [*Pickett et al.*, 2005]. The electron parameters, in particular, were obtained from detailed analysis of electron distribution functions obtained by the PEACE (Plasma Electron And Current Experiment) instrument on-board one of the four Cluster spacecraft (SC4) [*Johnstone et al.*, 1997]. These distribution functions are obtained, at best, every 2 s, which is not atypical for most space-based particle measurements. Considering that typical instabilities, such as the acoustic instability that can generate solitary waves of short time duration usually develop over only hundreds to thousands of plasma periods (order of 10s of ms or less for this specific case), it is not clear that those distribution functions provide the pre-unstable parameters necessary for carrying out an investigation. Certainly, these distribution functions will represent a composite of pre- and post-instability characteristics, assuming that the solitary waves were, in fact, generated during the time of the particle measurement. Given that solitary waves observed in the magnetosheath can propagate over distances at least as large as a km [*Pickett et al.*, 2010], it is not necessarily given that solitary waves observed in space are generated at the time and place of the measurement. However, it seems quite plausible to assume that they may be generated locally when observations show solitary waves of similar or sequential increasing/decreasing amplitudes spaced at discrete time intervals, such as the case well chosen by *Lakhina et al.* [2009, Figure 1].

[5] In spite of some of the measurement limitations and the lack of certainty of whether the solitary waves are generated locally, the theoretical studies of the acoustic model were extremely useful in showing that there exist steady state solutions of electrostatic solitary structures in four-component plasmas. We now take these studies one step further by examining the excitation of electrostatic waves in four-component plasmas and their nonlinear evolution by means of a self-consistent solution of the Vlasov-Poisson equations. We will use observed input parameters initially and then vary some of those parameters slightly in order to explore the possibility that we can infer the state of the unperturbed plasma and the resultant excitation that produces the observed solitary waves.

[6] This paper is structured as follows. Section 2 provides the model and the parameters used in the computer simulations. Section 3 presents the simulation results. Section 4 contains a summary of the computer simulation results together with a comparison of those results with spacecraft observations.

2. Simulation Model and Parameters

[7] In the present study, we solve spatiotemporal development of the complete position-velocity distribution function self-consistently based on the Vlasov equation together with the Poisson equation. The present numerical simulation code is a general 1x1v (one position dimension and one velocity dimension) Vlasov code with the ambient magnetic field taken along the simulation domain. We ignore electromagnetic perturbations so that the effects of the ambient magnetic field and electromagnetic waves are completely absent in the simulation domain. Then, the distribution function is reduced to the two-dimensional position-velocity phase space $f(x, v_x)$. The Vlasov simulation has significant benefit because numerical noise is suppressed substantially in comparison with one-dimensional electrostatic particle-in-cell simulations. The Vlasov code adopts the time-splitting algorithm [*Cheng and Knorr*, 1976] and a non-oscillatory, positive and conservative interpolation scheme for stable time-integration of phase-space distribution functions [*Umeda*, 2008b; *Umeda et al.*, 2012].

[8] Velocity distribution functions of the magnetosheath plasma are modeled first with four Maxwellian components [*Lakhina et al.*, 2009].

$$f(v_x) = \frac{n_s}{\sqrt{2\pi}V_{ts}} \exp\left[-\frac{(v_x - V_{ds})^2}{2V_{ts}^2}\right] \tag{1}$$

These components are core electrons (the subscript $s = ce$), an electron beam propagating parallel to the magnetic field ($s = pe$), an electron beam propagating antiparallel to the magnetic field ($s = ae$), and background ions ($s = i$). Simulation parameters for the present study are based on those listed in the paper by *Lakhina et al.* [2009], which were observed with the PEACE instrument [*Johnstone et al.*, 1997]. The normalized simulation parameters are listed in Table 1. Run 0 corresponds to "event 1" in the paper by *Lakhina et al.* [2009, Table 1]. Here, the plasma frequency ($\omega_{ps}^2 \equiv e^2 n_s/\epsilon_0 m_s$) is normalized to the total electron plasma frequency ($\omega_{pce}^2 + \omega_{ppe}^2 + \omega_{pae}^2 \equiv \omega_{pe}^2 = 1$), and the velocity is normalized to the thermal velocity of core electrons V_{tec}. The ions are assumed to have a realistic mass ratio $m_i/m_e = 1600$ with thermal energy of 100 eV.

[9] Although the initial velocity distribution function for Run 0 (i.e., the observed velocity distribution function) has a positive slope as shown by the dashed line in Figure 1 (bottom), the linear dispersion relation does not give unstable electron acoustic wave modes but rather gives only a stable Langmuir wave mode. There is also no wave growth in the Vlasov simulation for Run 0 (not shown). However, this is not surprising because a spacecraft sometimes observes distribution functions after saturation of microscopic instabilities and timescales for the saturation of electron-scale microscopic instabilities are sometimes shorter than the time resolution of particle instruments. In order to make the initial distribution functions unstable, we need to decrease the electron temperature.

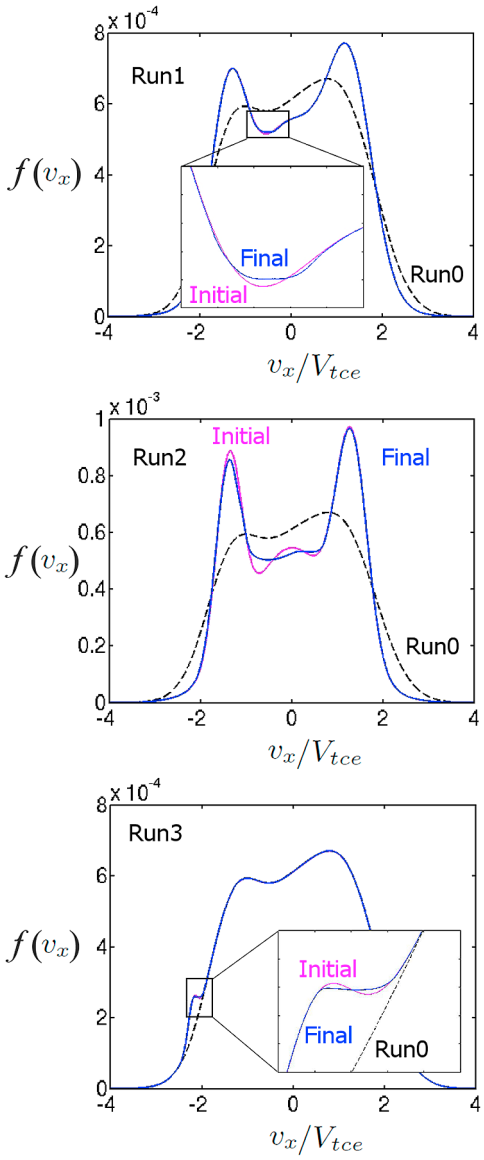

Figure 1. The electron velocity distribution functions at the initial and final ($\omega_{pe}t = 4000$) states for Runs 1–3. The electron velocity distribution function for Run 0 is also plotted with dashed lines for reference.

[10] In Runs 1 and 2, the temperatures of the two electron beams are set to be 0.5 and 0.25 of Run 0, respectively. The linear dispersion relations for Runs 1–2 are given in Figure 2. In all runs, the waves have phase velocities corresponding to the maximum positive gradient in the initial velocity distribution functions ($\partial f/\partial v_x$), which is consistent with the previous theoretical work [*Singh and Lakhina*, 2001]. There exists a wave with a positive growth rate only in the $-x$ direction in Run 1, while there exist waves with a positive growth rate in both the x and $-x$ directions in Run 2. The phase velocities of unstable modes in all runs are slower than the thermal velocity of the core electrons V_{tce} but faster than the thermal velocity of the beam electrons $V_{t(p,a)e}$. It should be noted that electron acoustic waves are generally defined in two-component plasmas consisting of hot and cold electrons at rest [e.g., *Ashour-Abdalla and Okuda*, 1986]. In the present study, on the other hand, there are two counter-streaming cold electron beams and one hot electron component at rest, which is a nonstandard situation for electron acoustic waves. It is obvious that unstable modes are neither electron beam modes nor ion acoustic modes because the phase velocities are much slower than the drift velocities of the two electron beams and the core electron temperature (45.8 eV) is smaller than the ion temperature. The phase velocities lie in the velocity range between V_{tce} and $V_{t(p,a)e}$, which indicates that the unstable wave modes correspond to electron acoustic waves.

[11] The number of spatial grid cells corresponds to $N_x = 2048$, and the number of velocity grid cells is chosen as $N_{v_x} = 4096$ over a velocity space that ranges from $v_{\max} = 10\ V_t$ to $v_{\min} = -10\ V_t$ for both electrons and ions. The grid spacing is equal to $\Delta x = 0.5\ V_{tec}/\omega_{pe}$ and the time step is equal to $\omega_{pe}t = 0.01$. Periodic boundary conditions are imposed in the x direction, while open boundary conditions are imposed in the v_x direction.

[12] In addition to simulations of four-component plasmas (Runs 0–2), we also perform a simulation with a five-component plasma (Run 3) consisting of a stable four-component plasma (Run 0) with a weak electron beam as a free energy source.

3. Results

[13] Figure 3 shows the spatial and temporal evolution of the electrostatic field E_x component for Runs 1 and 2. The position is normalized by V_{tce}/ω_{pe}, and the time is normalized by $1/\omega_{pe}$. The magnitude of electric field is normalized by $\omega_{pe}V_{tce}m_e/e$.

[14] A wave mode with a negative phase velocity is slowly excited in Run 1. The wave number at the maximum growth rate and the phase velocity are obtained as $k_x = -0.15$ and $v_p \sim -0.5\ V_{tce}$, respectively, from the linear analyses as shown in Figure 2, which is in quantitative agreement with the Vlasov simulation result in Figure 3a. The excited wave mode seems to coalesce with the neighboring one and becomes isolated, as discussed in the generation of electron phase-space holes [e.g., *Omura et al.*, 1996]. From Figure 3a, the phase velocity of the solitary structures is

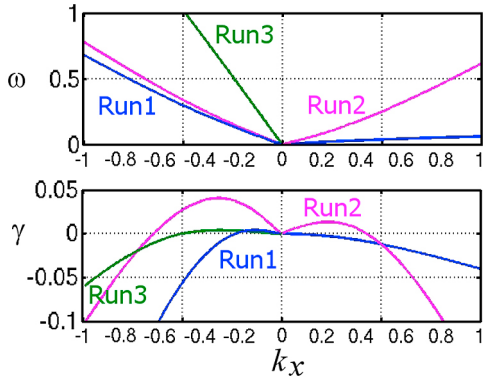

Figure 2. Linear dispersion relations for Runs 1–3. The frequency is normalized by ω_{pe} and the wave number is normalized by ω_{pe}/V_{tec}.

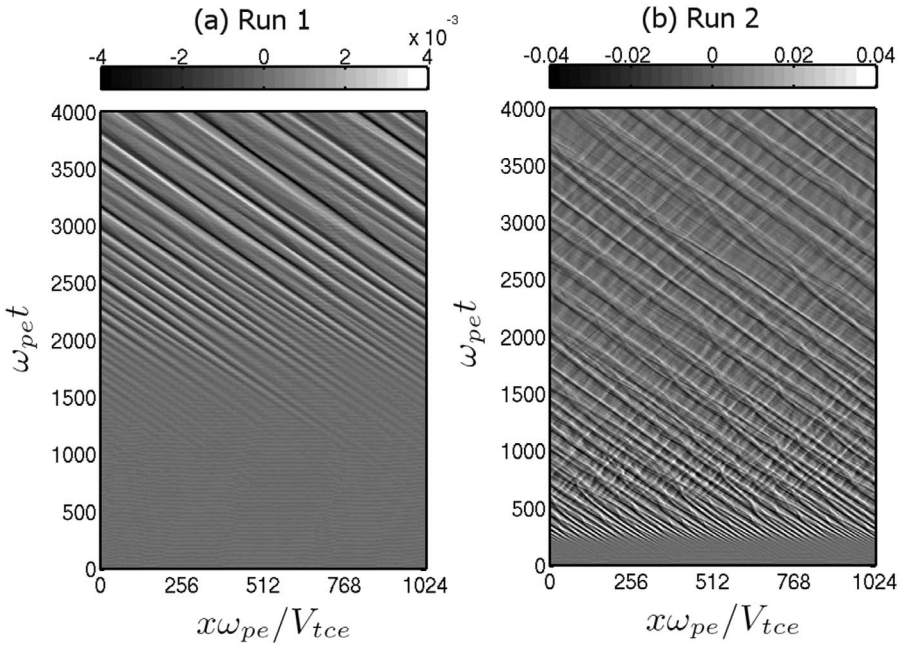

Figure 3. (a–b) Spatial and temporal evolution of electrostatic field E_x for Runs 1 and 2. The position is normalized by V_{tce}/ω_{pe}, and the time is normalized by $1/\omega_{pe}$. The magnitude of electric field is normalized by $\omega_{pe}V_{tce}m_e/e$.

estimated as $v_p \sim -0.45\ V_{tce}$, which is slightly slower than the phase velocity of the linearly unstable mode.

[15] The electric field profile in Figure 4a shows that the solitary structures have a positive electric field on the left-hand side and a negative electric field on the right-hand side. If an observer moves slower than the solitary structure, the polarization of the electric field $E_x(t)$ would turn from positive to negative, which indicates the existence of negative potentials. It is worth showing the electron phase space $f(x, v_x)$ and the corresponding waveforms of the electric field E_x component, potential ϕ and charge density ρ (Figure 4a). It is confirmed that there exist negative potentials and corresponding bipolar signatures of electric field. At the center of the negative potentials, the electron density is enhanced by

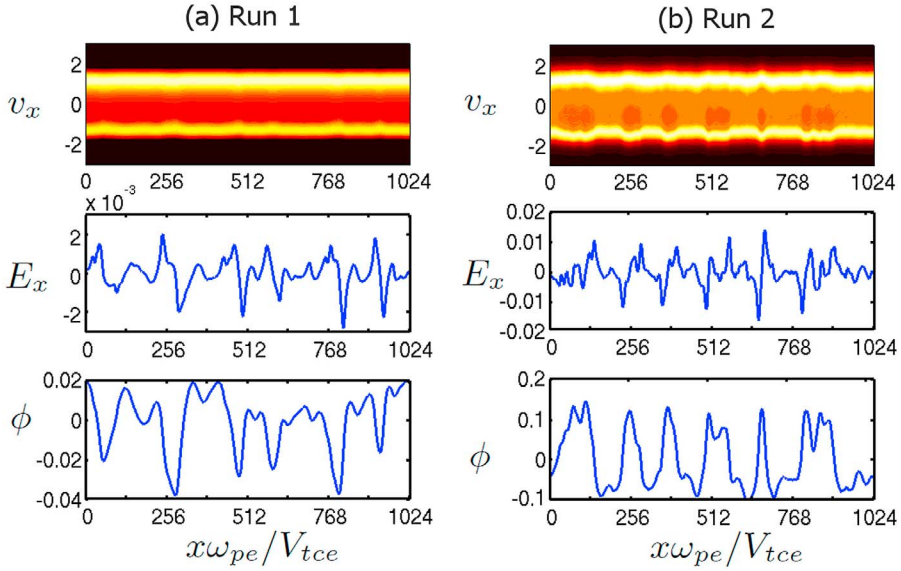

Figure 4. The electron phase space $f(x, v_x)$ and the corresponding waveforms of electric field E_x, potential ϕ and charge density ρ at $\omega_{pe}t = 4000$ in (a) Run 1 and (b) Run 2. The position is normalized by V_{tce}/ω_{pe}, and the velocity is normalized by V_{tce}. The magnitude of electric field is normalized by $\omega_{pe}V_{tce}m_e/e$, the magnitude of potential is normalized by $V_{tce}^2m_e/e$, and the magnitude of charge density is normalized by $\omega_{pe}^2m_e/e$.

Table 2. Characteristics of Electrostatic Solitary Structures Obtained in Runs 1–3[a]

Run	V	W	τ	E
1	0.45 $V_{tce} \sim$ 1280 km/s	150 $V_{tce}/\omega_{pe} \sim$ 2.2 km	150/$\omega_{pe} \sim$ 770 μs	0.002 $\omega_{pe}V_{tce}m_e/e \sim$ 6.3 mV/m
2	0.5 $V_{tce} \sim$ 1420 km/s	100 $V_{tce}/\omega_{pe} \sim$ 1.5 km	180/$\omega_{pe} \sim$ 920 μs	0.01 $\omega_{pe}V_{tce}m_e/e \sim$ 31.5 mV/m
3	2.1 $V_{tce} \sim$ 5960 km/s	50 $V_{tce}/\omega_{pe} \sim$ 0.7 km	24/$\omega_{pe} \sim$ 122 μs	0.0002 $\omega_{pe}V_{tce}m_e/e \sim$ 0.6 mV/m

[a]The quantities V, W, τ, and E denote the velocity, pulse width, pulse duration, and electric field intensity, respectively.

bunching of electrons in phase space. It is expected that the electrostatic solitary structures in Run 1 are electron acoustic solitary waves with negative potentials.

[16] In Run 2, wave modes are linearly excited in both the parallel and anti-parallel directions. Since waves with negative phase velocities have higher growth rates, these waves show the nonlinear development into solitary structures, while waves with positive phase velocities show a sinusoidal signature. The solitary structures propagating in the anti-parallel direction have bipolar waveforms turning from negative to positive as seen in Figure 3b, which indicates the existence of positive potentials. The formation of solitary structures is due to the coalescence of potential structures [e.g., *Omura et al.*, 1996].

[17] Figure 4b shows the electron phase space $f(x, v_x)$ and the corresponding waveforms of the electric field E_x component and potential ϕ in Run 2. It is confirmed that there exist electron phase-space holes with positive potentials and corresponding bipolar signatures of electric field.

[18] In Figure 1, we plotted the electron velocity distribution function at the final stage ($\omega_{pe}t$ = 4000) in Runs 1 and 2. The final electron velocity distribution functions in Runs 1 and 2 show strong double peaks and are different from the observed velocity distribution function (Run 0). However, the nonlinear evolution of these two runs is very different. Electron acoustic solitary waves with negative potential exist in Run 1, while electron phase-space holes exist in Run 2. The final distribution function in Run 1 is almost the same as the initial electron velocity distribution function with a minor modification at $v_x/V_{tce} \sim 0.5$. The final distribution function in Run 2 shows a modification for $v_x < 0$.

[19] We can estimate the characteristics of electrostatic solitary structures in the Vlasov simulations with $V_{tce} \sim$ 2840 km/s and $\omega_{pe}/2\pi \sim$ 31 kHz. Table 2 shows the characteristics of electrostatic solitary structures obtained in our simulation runs. We found that electrostatic solitary structures generated in the four-component plasma (Runs 1 and 2) have longer duration times (or slower propagation speeds) and higher wave amplitudes than the solitary structures observed in the magnetosheath (Event 1 in Table 3 by *Lakhina et al.* [2009]).

[20] It should be noted that Table 3 by *Lakhina et al.* [2009] was obtained as analytic solutions to the fluid equations for the four-component plasmas that could explain the characteristics of electrostatic solitary structures observed by the Cluster spacecraft. However, the propagation speed of electrostatic solitary structures obtained in their theoretical analysis is faster (~6000 km/s) than the drift velocities of the two beam components and the thermal velocities of the three (one core and two beam) components. Such high-speed electrostatic solitary structures cannot be excited in the four-component plasma assumed by *Lakhina et al.* [2009], because an electrostatic instability takes place at a phase velocity v_p where the maximum positive gradient in a velocity distribution function is given (see the velocity distribution functions in Figure 1 and the linear dispersion relations in Figure 2). Also, the electrostatic potential energy of solitary structures estimated by *Lakhina et al.* [2009] is much lower (1–5%) than the thermal energy of core electrons. This suggests that we might need an additional high-speed but weak free energy source (a positive gradient of velocity distribution function) at $|v_x| \sim 2\ V_{tce}$. One of candidate generation mechanisms for generating electrostatic solitary structures with a higher propagation speed and a small amplitude is the bump-on-tail instability [e.g., *Omura et al.*, 1996] where electrostatic waves are excited by a high-speed and low-density electron beam.

[21] In addition to Runs 1 and 2, we performed a simulation run of a five-component plasma (Run 3). The initial velocity distribution consists of the observed (stable) velocity distribution consisting of the four components (Run 0) with a weak electron beam as a high-speed free energy source. The velocity distribution becomes unstable to the well-known bump-on-tail instability [*Omura et al.*, 1996]. Figure 5 shows the electron phase space $f(x, v_x)$ and the corresponding waveforms of the electric field E_x component and potential ϕ in Run 3 with the same format as Figure 4.

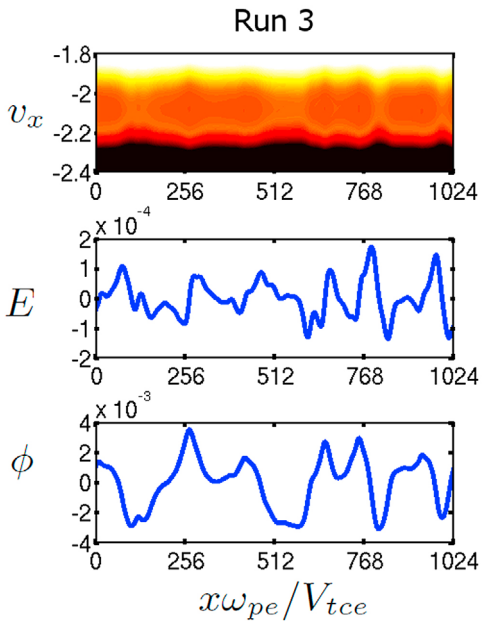

Figure 5. The electron phase space $f(x, v_x)$ and the corresponding waveforms of electric field E_x and potential ϕ at $\omega_{pe}t$ = 25,000 in Run 3. The position is normalized by V_{tce}/ω_{pe}, and the velocity is normalized by V_{db}. The magnitude of electric field is normalized by $\omega_{pe}V_{tce}m_e/e$, and the magnitude of potential is normalized by $V_{tce}^2m_e/e$.

[22] We see that electron phase-space holes are excited in a narrow velocity range between $-1.9\ V_{tce}$ and $-2.2\ V_{tce}$. The velocity distribution function is also modified in the narrow velocity range (see Figure 1). Such a small velocity space enhancement might be hardly observed by particle instruments [e.g., *Omura et al.*, 1999].

[23] We estimated the characteristics of the electron phase-space holes (see Table 2), and found that the velocity, pulse width, pulse duration, and electric field of electrostatic solitary structures (electron phase-space holes) excited by the bump-on-tail instability are more similar to the analytic solution of the electron acoustic solitary waves obtained by *Lakhina et al.* [2009], which is also consistent with the amplitude and duration time of bipolar solitary pulses observed by the Cluster spacecraft.

4. Summary

[24] Using a one-dimensional electrostatic Vlasov simulation, we studied the nonlinear evolution of a four-component plasma consisting of one core electron component, two electron beams drifting in parallel and anti-parallel directions, and one background ion component. Although the simulation parameters are based on Cluster observations made in the magnetosheath [*Lakhina et al.*, 2009], the parameters have been slightly changed from the observations.

[25] The present study is summarized as follows:

[26] 1. The linear dispersion relation for the observed velocity distribution function (Run 0) [*Lakhina et al.*, 2009] does not show positive growth rate. The Vlasov simulation also does not show wave growth. Thus the initial velocity distribution functions for the Vlasov simulation are modified from the observed ones in order to make them unstable.

[27] 2. When the temperatures of the two (parallel and anti-parallel) electron beams are decreased slightly from the observed ones, the linear dispersion relation shows a positive growth rate only in the anti-parallel direction (Run 1). The Vlasov simulation shows that electrostatic solitary structures with negative potentials are formed in the nonlinear evolution. We expect that the solitary structures correspond to electron acoustic solitary waves with negative potential that propagate in the anti-parallel direction.

[28] 3. When the temperatures of the two electron beams are decreased even more, the linear dispersion relation for the velocity distribution function shows a positive growth rate in both the parallel and anti-parallel directions (Run 2). The Vlasov simulation shows that electrostatic solitary structures with positive potentials are formed in the nonlinear stage of evolution which correspond to electron phase-space holes [e.g., *Omura et al.*, 1996].

[29] 4. Duration times and wave amplitudes of electrostatic solitary structures generated in the four-component plasma are longer and higher than the solitary structures observed by the Cluster spacecraft in the magnetosheath.

[30] 5. Duration times and wave amplitudes of electrostatic solitary structures generated by the bump-on-tail instability are in better agreement with the Cluster observation.

[31] It is worth noting that the characteristics of solitary structures generated by the bump-on-tail instability (Run 3) are similar to those of the electron acoustic solitary structures [*Lakhina et al.*, 2009], because phase-space holes correspond to phase-space structures of the weak electron beam (fifth component) while the other three electron components lead to the generation of density decreases and enhancements which can be described by the multifluid equations. However, it is difficult to prove the existence of the "fifth" component because a small velocity space enhancement due to a weak electron beam might be hardly observed by particle instruments [e.g., *Omura et al.*, 1999].

[32] Finally, it should be noted that densities and magnetic fields in the magnetosheath is highly turbulent [*Retino et al.*, 2007]. In the present study, however, we assume that the background ions and magnetic fields are constant because we focus on an electron-scale micro-instability on a time-scale of $\omega_{pe}t \sim 25{,}000$ which correspond to $\omega_{ci}t \sim 2$ in the magnetosheath. Large-scale fluctuations can easily change the types of micro-instabilities, and a large-scale multidimensional simulation is necessary.

[33] **Acknowledgments.** The computer simulations were carried out as a computational joint research program at STEL, Nagoya University and RISH, Kyoto University. T.U. acknowledges support from MEXT/JSPS under grant-in-aid (KAKENHI) 21740352 and 23740367. M.A.A. acknowledges support from NASA Goddard Space Flight Center under grant NNX08AO48G. J.S.P. acknowledges support from NASA Goddard Space Flight Center under grant NNX07AI24G. M.L.G. acknowledges support from NASA Goddard Space Flight Center under grant NNX10AQ47G.

[34] Philippa Browning thanks the reviewers for their assistance in evaluating this paper.

References

Ashour-Abdalla, M., and H. Okuda (1986), Electron acoustic instabilities in the geomagnetic tail, *Geophys. Res. Lett.*, *13*, 366–369, doi:10.1029/GL013i004p00366.

Bale, S. D., P. J. Kellogg, D. E. Larson, R. P. Lin, K. Goetz, and R. P. Lepping (1998), Bipolar electrostatic structures in the shock transition region: Evidence of electron phase space holes, *Geophys. Res. Lett.*, *25*, 2929–2932.

Bernstein, I. B., J. M. Greene, and M. D. Kruskal (1957), Exact nonlinear plasma oscillations, *Phys. Rev.*, *108*, 546–550.

Cattell, C., J. Crumley, J. Dombeck, J. Wygant, and F. S. Mozer (2002), Polar observations of solitary waves at the Earth's magnetopause, *Geophys. Res. Lett.*, *29*(5), 1065, doi:10.1029/2001GL014046.

Cattell, C., et al. (2005), Cluster observations of electron holes in association with magnetotail reconnection and comparison to simulations, *J. Geophys. Res.*, *110*, A01211, doi:10.1029/2004JA010519.

Chen, L.-J., and G. K. Parks (2002), BGK electron solitary waves in 3D magnetized plasma, *Geophys. Res. Lett.*, *29*(9), 1331, doi:10.1029/2001GL013385.

Chen, L.-J., D. J. Thouless, and J.-M. Tang (2004), Bernstein-Greene-Kruskal solitary waves in three-dimensional magnetized plasma, *Phys. Rev. E*, *69*, 055401.

Cheng, C. Z., and G. Knorr (1976), The integration of the Vlasov equation in configuration space, *J. Comput. Phys.*, *22*, 330–351.

Ergun, R. E., C. W. Carlson, J. P. McFadden, F. S. Mozer, L. Muschietti, I. Roth, and R. Strangeway (1998), Debye-scale plasma structures associated with magnetic-field-aligned electric field, *Phys. Rev. Lett.*, *81*, 826–829.

Ghosh, S. S., J. S. Pickett, G. S. Lakhina, J. D. Winningham, and B. Lavraud (2008), Parametric analysis of positive amplitude electron acoustic solitary waves in a magnetized plasma and its application to boundary layers, *J. Geophys. Res.*, *113*, A06218, doi:10.1029/2007JA012768.

Franz, J. R., P. M. Kintner, and J. S. Pickett (1998), POLAR observations of coherent electric field structures, *Geophys. Res. Lett.*, *25*, 1277–1280.

Goldman, M. V., M. M. Oppenheim, and D. L. Newman (1999), Nonlinear two-stream instabilities as an explanation for auroral bipolar wave structures, *Geophys. Res. Lett.*, *26*, 1821–1824.

Johnstone, A. D., et al. (1997), PEACE: A plasma electron and current experiment, *Space Sci. Rev.*, *79*, 351–398.

Kojima, H., H. Matsumoto, S. Chikuba, S. Horiyama, M. Ashour-Abdalla, and R. R. Anderson (1997), Geotail waveform observations of broadband/narrowband electrostatic noise in the distant tail, *J. Geophys. Res.*, *102*, 14,439–14,455.

Krasovsky, V. L., H. Matsumoto, and Y. Omura (1997), Bernstein-Greene-Kruskal analysis of electrostatic solitary waves observed with Geotail, *J. Geophys. Res.*, *102*, 22,131–22,139.

Krasovsky, V. L., H. Matsumoto, and Y. Omura (2003), Electrostatic solitary waves as collective charges in a magnetospheric plasma: Physical structure and properties of Bernstein-Greene-Kruskal (BGK) solitons, *J. Geophys. Res.*, *108*(A3), 1117, doi:10.1029/2001JA000277.

Lakhina, G. S., S. V. Singh, A. P. Kakad, F. Verheest, and R. Bharuthram (2008), Study of nonlinear ion- and electron-acoustic waves in multicomponent space plasmas, *Nonlinear Processes Geophys.*, *15*, 903–913.

Lakhina, G. S., S. V. Singh, A. P. Kakad, M. L. Goldstein, A. F. Vinas, and J. S. Pickett (2009), A mechanism for electrostatic solitary structures in the Earth's magnetosheath, *J. Geophys. Res.*, *114*, A09212, doi:10.1029/2009JA014306.

Matsumoto, H., H. Kojima, T. Miyatake, Y. Omura, M. Okada, I. Nagano, and M. Tsutsui (1994), Electrostatic solitary waves (ESW) in the magnetotail: BEN wave forms observed by GEOTAIL, *Geophys. Res. Lett.*, *21*, 2915–2918.

Miyake, T., Y. Omura, H. Matsumoto, and H. Kojima (1998), Two-dimensional computer simulations of electrostatic solitary waves observed by Geotail spacecraft, *J. Geophys. Res.*, *103*, 11,841–11,850.

Miyake, T., Y. Omura, and H. Matsumoto (2000), Electrostatic particle simulations of solitary waves in the auroral region, *J. Geophys. Res.*, *105*, 23,239–23,249.

Mozer, F. S., R. Ergun, M. Temerin, C. Cattell, J. Dombeck, and J. Wygant (1997), New features of time domain electric-field structures in the auroral acceleration region, *Phys. Rev. Lett.*, *79*, 1281–1284.

Omura, Y., H. Matsumoto, T. Miyake, and H. Kojima (1996), Electron beam instabilities as generation mechanism of electrostatic solitary waves in the magnetotail, *J. Geophys. Res.*, *101*, 2685–2697.

Omura, Y., H. Kojima, N. Miki, T. Mukai, H. Matsumoto, and R. Anderson (1999), Electrostatic solitary waves carried by diffused electron beams observed by the Geotail spacecraft, *J. Geophys. Res.*, *104*, 14,627–14,637, doi:10.1029/1999JA900103.

Oppenheim, M. M., G. Vetoulis, D. L. Newman, and M. V. Goldman (2001), Evolution of electron phase-space holes in 3D, *Geophys. Res. Lett.*, *28*, 1891–1894.

Pickett, J. S., J. D. Menietti, D. A. Gurnett, B. T. Tsurutani, P. Kintner, E. Klatt, and A. Balogh (2003), Solitary potential structures observed in the magnetosheath by the Cluster spacecraft, *Nonlinear Processes Geophys.*, *10*, 3–11.

Pickett, J. S., et al. (2005), On the generation of solitary waves observed by Cluster in the near-Earth magnetosheath, *Nonlinear Processes Geophys.*, *12*, 181–193.

Pickett, J. S., et al. (2010), On the propagation and modulation of electrostatic solitary waves observed near the magnetopause on Cluster, in *Modern Challenges in Nonlinear Plasma Physics: A Festchrift Honoring the Career of Dennis Papadopoulos*, edited by D. Vassiliadis et al., *AIP Conf. Proc.*, *1320*, 115–124.

Retino, A., D. Sundkvist, A. Vaivads, F. Mozer, M. Andre, and C. J. Owen (2007), In situ evidence of magnetic reconnection in turbulent plasma, *Nature Phys.*, *3*, 235–238.

Singh, N., S. M. Loo, B. E. Wells, and C. Deverpalli (2000), Three-dimensional structure of electron holes driven by an electron beam, *Geophys. Res. Lett.*, *27*, 2469–2472.

Singh, S. V., and G. S. Lakhina (2001), Generation of electron-acoustic waves in the magnetosphere, *Planet. Space Sci.*, *49*, 107–114.

Umeda, T. (2008a), Generation of low-frequency electrostatic and electromagnetic waves as nonlinear consequences of beam-plasma interactions, *Phys. Plasmas*, *15*, 064502.

Umeda, T. (2008b), A conservative and non-oscillatory scheme for Vlasov code simulations, *Earth Planets Space*, *60*, 773–779.

Umeda, T., Y. Omura, H. Matsumoto, and H. Usui (2002), Formation of electrostatic solitary waves in space plasmas: Particle simulations with open boundary conditions, *J. Geophys. Res.*, *107*(A12), 1449, doi:10.1029/2001JA000286.

Umeda, T., Y. Omura, and H. Matsumoto (2004), Two-dimensional particle simulation of electromagnetic field signature associated with electrostatic solitary waves, *J. Geophys. Res.*, *109*, A02207, doi:10.1029/2003JA010000.

Umeda, T., Y. Omura, T. Miyake, H. Matsumoto, and M. Ashour-Abdalla (2006), Nonlinear evolution of the electron two-stream instability: Two-dimensional particle simulations, *J. Geophys. Res.*, *111*, A10206, doi:10.1029/2006JA011762.

Umeda, T., Y. Nariyuki, and D. Kariya (2012), A non-oscillatory and conservative semi-Lagrangian scheme with fourth-degree polynomial interpolation for solving the Vlasov equation, *Comput. Phys. Commun.*, *183*, 1094–1100, doi:10.1016/j.cpc.2012.01.011.